they were put through one of four sequences of rotations—left then CCW, CCW then left, right then CW, or CW then right—each repeated a total of 10 times in randomly ordered blocks of 5. All rotations were about the centre of the subject's head. Horizontal rotations were 60° and lasted 1.5 s, torsional rotations were 10° and lasted 0.75 s. With a 0.35-s pause between turns, each sequence of two rotations lasted 2.6 s, and was followed by 4 s stationary in darkness. Starting positions were chosen so that all horizontal rotations had earth-vertical axes, and so did not change the subject's orientation relative to gravity. This arrangement shows that gravity sensors cannot remove the need for non-commutative computations in the VOR: to keep the eyes on target, any gravity-based estimates of the subject's torsional rotation must be combined with other estimates of the horizontal rotation[25,26], and this combination must be non-commutative, if the eyes are to end up in distinct positions as in Fig. 3.

Eye movements. We recorded the position of the left eye 100 times per second using search coils[27]. For analysis, we omitted all trials where saccades (sudden gaze shifts) occurred during the head rotations. All data figures and simulations express eye positions as gaze vectors, showing the horizontal and vertical components of a vector of length one that points forward along the gaze line.

Simulations. Figure 2 shows the predictions of Raphan's vector-pulley model of the VOR[19], with $k_\phi = 0.25$. Vertical excursions in the figure are small owing to the model's low torsional gain and errors in its vertical eye-position commands. These errors show up even in the rotation between positions 1 and 2 because the eye starts at 30° left and the model does not correctly handle the non-commutative interaction with the preceding rotation(s) that brought the eye there. The non-commutative model described in the text is simplified from the one in ref. 5: both models match Figs 1c and 3, but the former used a four-component neural representation of eye position and no pulleys, whereas the present one uses three components and the linear-plant model[12] of the eye muscles, which is a simple way to model pulleys[12–14,21]. The full equations for this non-commutative VOR model are: $e = -h - h \times x$, $dx/dt = e$, $m = kx + re$, $dq/dt = (m - kq)/r$. Here k and r are related to the stiffness and viscosity of the orbital tissues[6,24]. All other variables are three-component vectors: q is eye position, m is motor-neuron activity, x is the eye-position command in the brainstem, h is the head-velocity signal from the inner ear, e is a command from vestibular nuclei to motor neurons, and $\times$ is the vector cross product. The model is simple and biologically plausible, requiring only scalar integration, addition, subtraction and multiplication, all of which are believed to be in the repertoire of neurons[28]. The formula for e implies that VOR circuits are cross-coupled, with vertical head-velocity signals influencing horizontal eye-position commands, and so on. Such cross-connections are also indicated by experiments in which the VOR was trained to produce eye movements about one axis in response to head motion about an orthogonal axis[29,30].

Received 2 December 1998; accepted 30 March 1999.

1. Hamilton, W. R. *Lectures on Quaternions* (Hodges, Dublin, 1853).
2. Schutz, B. *Geometrical Methods of Mathematical Physics* (Cambridge Univ. Press, Cambridge, 1980).
3. McCarthy, J. M. *An Introduction to Theoretical Kinematics* (North-Holland, Amsterdam, 1990).
4. Westheimer, G. Kinematics of the eye. *J. Opt. Soc. Am.* **47,** 967–974 (1957).
5. Tweed, D. & Vilis, T. Implications of rotational kinematics for the oculomotor system in three dimensions. *J. Neurophysiol.* **58,** 832–849 (1987).
6. Carpenter, R. H. S. *The Movements of the Eyes* (Pion, London, 1988).
7. Tweed, D. & Vilis, T. Geometric relations of eye position and velocity vectors during saccades. *Vision Res.* **30,** 111–127 (1990).
8. Crawford, J. D. & Vilis, T. Axes of eye rotation and Listing's law during rotation of the head. *J. Neurophysiol.* **65,** 407–423 (1991).
9. Minken, A. W. H., van Opstal, A. J. & Van Gisbergen, J. A. M. Three-dimensional analysis of strongly curved saccades elicited by double-step stimuli. *Exp. Brain Res.* **93,** 521–533 (1993).
10. Hestenes, D. Invariant body kinematics I. Saccadic and compensatory eye movements. *Neural Netw.* **7,** 65–77 (1994).
11. Hestenes, D. Invariant body kinematics: II. Reaching and neurogeometry. *Neural. Netw.* **7,** 79–88 (1994).
12. Tweed, D., Misslisch, H. & Fetter, M. Testing models of the oculomotor velocity-to-position transformation. *J. Neurophysiol.* **72,** 1425–1429 (1994).
13. Smith, M. A. & Crawford, J. D. Neural control of rotational kinematics within realistic vestibuloocular coordinate systems. *J. Neurophysiol.* **80,** 2295–2315 (1998).
14. Tweed, D. A three-dimensional model of the human eye-head saccadic system. *J. Neurophysiol.* **77,** 654–666 (1997).
15. Henriques, D. Y. P., Klier, E. M., Smith, M. A., Lowy, D. & Crawford, J. D. Gaze centered remapping of remembered visual space in an open-loop pointing task. *J. Neurosci.* **18,** 1583–1594 (1998).
16. Van Opstal, A. J., Hepp, K., Hess, B. J. M., Straumann, D. & Henn, V. Two- rather than three-dimensional representation of saccades in monkey superior colliculus. *Science* **252,** 1313–1315 (1991).
17. Schnabolk, C. & Raphan, T. Modeling three-dimensional velocity-to-position transformation in oculomotor control. *J. Neurophysiol.* **71,** 623–638 (1994).
18. Straumann, D., Zee, D. S., Solomon, D., Lasker, A. G. & Roberts, D. Transient torsion during and after saccades. *Vision Res.* **35,** 3321–3334 (1995).
19. Raphan, T. In *Three-dimensional Kinematics of Eye, Head and Limb Movements* (eds Fetter, M., Haslwanter, T., Misslisch, H. & Tweed, D.) 359–376 (Harwood, Amsterdam, 1997).
20. Raphan, T. Modeling control of eye orientation in three dimensions. I. Role of muscle pulleys in determining saccadic trajectory. *J. Neurophysiol.* **79,** 2653–2667 (1998).
21. Quaia, C. & Optican, L. M. Commutative saccadic generator is sufficient to control a 3-d ocular plant with pulleys. *J. Neurophysiol.* **79,** 3197–3215 (1998).
22. Miller, J. M., Demer, J. L. & Rosenbaum, A. L. Effect of transposition surgery on rectus muscle paths by magnetic resonance imaging. *Ophthalmology* **100,** 475–487 (1993).
23. Demer, J. L., Miller, J. M. & Poukens, V. Surgical implications of the rectus extraocular muscle pulleys. *J. Pediatr. Ophthalmol. Strabismus* **33,** 208–218 (1996).
24. Robinson, D. A. Oculomotor unit behavior in the monkey. *J. Neurophysiol.* **35,** 393–404 (1970).
25. Glasauer, S. Interaction of semicircular canals and otoliths in the processing structure of the subjective zenith. *Ann. NY Acad. Sci.* **656,** 847–849 (1992).
26. Merfeld, D. M. Modeling the vestibulo-ocular reflex of the squirrel monkey during eccentric rotation and roll tilt. *Exp. Brain Res.* **106,** 123–134 (1995).
27. Robinson, D. A. A method of measuring eye movement using a scleral search coil in a magnetic field. *IEEE Trans. Biomed. Eng.* **10,** 137–145 (1963).
28. Koch, C. Biophysics of Computation: Information Processing in Single Neurons 471–473 (Oxford Univ. Press, New York, 1999).
29. Schultheis, L. W. & Robinson, D. A. Directional plasticity of the vestibuloocular reflex in the cat. *Ann. NY Acad. Sci.* **374,** 504–512 (1981).
30. Peng, G. C., Baker, J. F. & Peterson, B. W. Dynamics of directional plasticity in the human vertical vestibulo-ocular reflex. *J. Vestib. Res.* **4,** 453–460 (1994).

Acknowledgements. We thank D. M. Broussard, J. D. Crawford, J. Dichgans, C. E. Hawkins, J. A. Sharpe and T. Vilis for comments on the manuscript. This work was supported by the MRC of Canada and the Deutsche Forschungsgemeinschaft.

Correspondence and requests for materials should be addressed to D.B.T.

Inhibition of caspase-1 slows disease progression in a mouse model of Huntington's disease

Victor O. Ona*, Mingwei Li*, Jean Paul G. Vonsattel†, L. John Andrews*, Sohail Q. Khan*, Woosik M. Chung‡, Ariel S. Frey‡, Anil S. Menon‡, Xiao-Jiang Li§, Philip E. Stieg*, Junying Yuan‖, John B. Penney‡, Anne B. Young‡, Jang-Ho J. Cha‡ & Robert M. Friedlander*¶

* *Neurosurgical Service, Department of Surgery, Brigham and Women's Hospital, Harvard Medical School, Boston, Massachusetts 02115, USA*
† *Department of Neuropathology, Massachusetts General Hospital, Harvard Medical School, Boston, Massachusetts 02114, USA*
‡ *Department of Neurology, Massachusetts General Hospital, Harvard Medical School, Boston, Massachusetts 02114, USA*
§ *Department of Genetics, Emory University School of Medicine, Atlanta, Georgia 30322, USA*
‖ *Department of Cell Biology, Harvard Medical School, Boston, Massachusetts 02115, USA*

Huntington's disease is an autosomal-dominant progressive neurodegenerative disorder resulting in specific neuronal loss and dysfunction in the striatum and cortex[1]. The disease is universally fatal, with a mean survival following onset of 15–20 years and, at present, there is no effective treatment. The mutation in patients with Huntington's disease is an expanded CAG/polyglutamine repeat in huntingtin, a protein of unknown function with a relative molecular mass of 350,000 (M_r 350K)[2]. The length of the CAG/polyglutamine repeat is inversely correlated with the age of disease onset. The molecular pathways mediating the neuropathology of Huntington's disease are poorly understood. Transgenic mice expressing exon 1 of the human *huntingtin* gene with an expanded CAG/polyglutamine repeat develop a progressive syndrome with many of the characteristics of human Huntington's disease[3]. Here we demonstrate evidence of caspase-1 activation in the brains of mice and humans with the disease. In this transgenic mouse model of Huntington's disease, expression of a dominant-negative caspase-1 mutant extends survival and delays the appearance of neuronal inclusions, neurotransmitter receptor alterations and onset of symptoms, indicating that

caspase-1 is important in the pathogenesis of the disease. In addition, we demonstrate that intracerebroventricular administration of a caspase inhibitor delays disease progression and mortality in the mouse model of Huntington's disease.

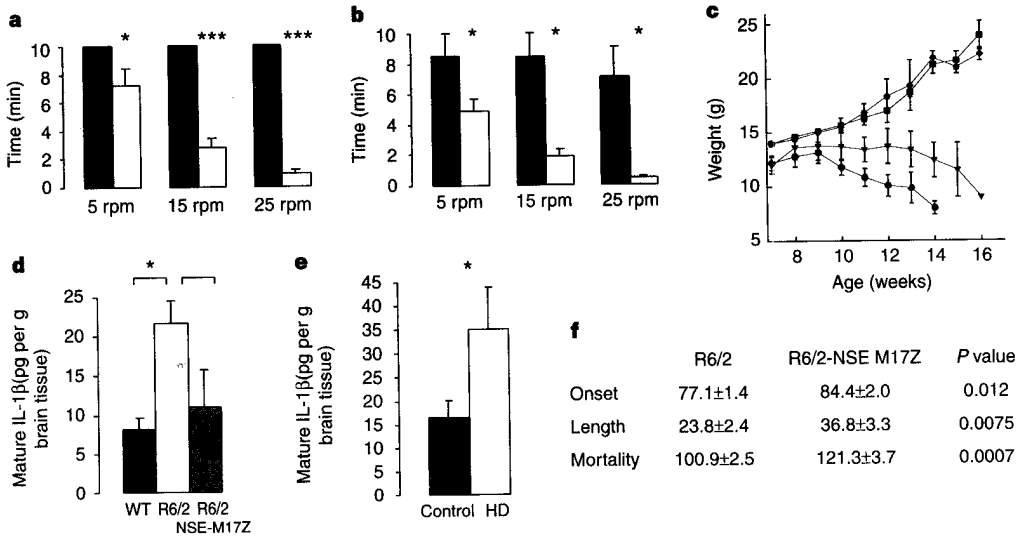
Transgenic mice expressing exon 1 of human *huntingtin* with expanded CAG/polyglutamine repeat lengths under the control of its endogenous promoter develop a progressive, ultimately fatal neurological phenotype with many features of human Huntington's disease[3]. Of these transgenic mouse lines, the R6/2 line has been the most thoroughly studied[3–5]. R6/2 mice develop normally, but by 5–7 weeks of age show significant loss of brain and body weight compared to control wild-type mice[3,4]. Features of juvenile Huntington's disease, including irregular gait, abrupt shuddering movements, resting tremors and epileptic seizures, begin at about nine weeks of age. Ubiquitinated neuronal intranuclear inclusions (NII) can be found in striatal neurons of R6/2 mice by four weeks of age[4]. NII have also been found in the brains of human Huntington's disease patients[6], but the role of NII in the pathogenesis of Huntington's disease is unknown.

The caspases are a family of cysteine proteases that are important for regulating apoptosis[7]. To evaluate a possible role for caspases in Huntington's disease, we crossbred R6/2 mice with a well characterized transgenic mouse expressing a dominant-negative mutant of caspase-1 in the brain[8]. In the mutant caspase-1 protein (M17Z), the active-site cysteine is substituted with a glycine. The neuron-specific enolase promoter targets the expression of mutant caspase-1 to neurons and glia within the central nervous system (NSE M17Z)[9,10]. The M17Z protein can act as a dominant-negative inhibitor of caspase-1 pathways, as demonstrated by inhibiting lipopolysaccharide- and cerebral ischaemia-mediated pro-interleukin-1β (pro-IL-1β) processing[8,11]. However, the mutant caspase-1 protein might also affect caspases other than caspase-1. The NSE M17Z mouse has normal embryonic development and brain size, and has been used as a tool to evaluate the role of caspase-1-mediated cell death in cerebral ischaemia and in amyotrophic lateral sclerosis (ALS)[8,12]. Decreased infarct size following ischaemia and delayed progression of ALS have been demonstrated in the NSE M17Z mouse.

R6/2 and R6/2-NSE M17Z mice develop normally and are indistinguishable from their wild-type littermates until about seven weeks of age. Progression of motor dysfunction was objectively evaluated using a RotaRod. R6/2-NSE M17Z mice performed significantly better than R6/2 mice throughout the test period (Fig. 1a). The deterioration of motor coordination seen in R6/2 mice is also seen in R6/2-NSE M17Z mice at a later stage (Fig. 1b). These results show that expression of the caspase-1 mutant delays the progression of motor dysfunction in R6/2 mice. To verify that the differences were not due to different levels of mutant *huntingtin* transgene expression in R6/2 and R6/2-NSE M17Z mice, we performed quantitative *in situ* hybridization. Equal expression was detected in R6/2 and R6/2-NSE M17Z mice. There was no transgene expression in either wild-type or NSE M17Z mice (data not shown).

Huntington's disease patients show significant weight loss despite adequate caloric intake, indicating a hypermetabolic state[1]. The aetiology of weight loss and hypermetabolism are unknown, and they do not appear to result solely from hyperkinesia. Similarly, R6/2 mice gain weight normally up to 6–7 weeks of age, and thereafter progressively lose weight to about 60% of that of controls[3]. The weight curve of R6/2-NSE M17Z mice is intermediate between those of control and R6/2 mice. In addition, the weight of the R6/2-NSE M17Z mice does not decrease to the same level before death as in their R6/2 counterparts (12.4 g versus 8.8 g, $P < 0.05$) (Fig. 1c). NSE-M17Z mice weighed the same as wild-type mice. As the NSE promoter targets transgene expression to the brain and testis, these results indicate that weight loss in R6/2 mice results partly from a systemic manifestation of disease progression within the nervous system[9]. However, as mutant huntingtin is expressed in peripheral tissues, low levels of M17Z expression might affect a putative role for peripheral huntingtin as a mediator of weight loss[3].

Elevation of mature IL-1β levels has been used as sensitive and specific evidence for caspase-1 activation, as caspase-1 is the main (if not the only) enzyme to activate pro-IL-1β *in vivo*[13]. To evaluate caspase-1 activation in R6/2 mice, we measured mature IL-1β in brain lysate of 12-week-old symptomatic mice. Levels of mature IL-1β in R6/2 mice were elevated to 268% of those in wild-type controls ($P = 0.007$). The increase in mature IL-1β was signifi-



f

	R6/2	R6/2-NSE M17Z	*P* value
Onset	77.1±1.4	84.4±2.0	0.012
Length	23.8±2.4	36.8±3.3	0.0075
Mortality	100.9±2.5	121.3±3.7	0.0007

Figure 1 Progression of disease in R6/2 mice is mediated by a caspase-1-dominant-negative-sensitive pathway. **a**, Nine-, and **b**, twelve-week-old mice were tested on a RotaRod (Columbus Instruments) at three speeds. Testing was terminated either when the mouse fell from the rod or at 10 min if it remained on the rod. Black bars, R6/2-NSE M17Z; white bars, R6/2 mice. rpm, rotations per minute. **c**, Body weight. Female mice of the indicated genotypes were used to generate weight curves (n = 6–8 per group). Squares, wild type; diamonds, NSE M17Z; circles, R6/2; triangles, R6/2-NSE M17Z. **d**, Mature IL-1β levels in 12-week-old mice ($n = 4$). **e**, Mature IL-1β levels in grade 3-4 patients (HD) ($n = 5$) and control brains ($n = 6$). **f**, Disease onset, length and mortality in days are recorded as mean ± s.e.m. Complete consecutive litters of the same generation were used for this part of the study. R6/2, $n = 14$; R6/2-NSE M17Z, $n = 7$. Error bars indicate s.e.m. Asterisk, $P < 0.05$; three asterisks, $P < 0.0005$.

cantly inhibited in 12-week-old R6/2-NSE M17Z mice (Fig. 1d). Mature IL-1β was not raised in eight-week-old asymptomatic R6/2 mice. Thus, the increase in mature IL-1β in symptomatic R6/2 mice is inhibited in caspase-1 dominant-negative mutants. To evaluate the relevance of this finding, we measured mature IL-1β levels in brains of human patients. In human grade 3–4 Huntington's disease cortex, mature IL-1β was significantly increased to 213% of that in normal controls ($P < 0.05$) (Fig. 1e).

To evaluate the impact of caspase-1 dominant-negative inhibition on Huntington's disease, we monitored disease progression in R6/2 and R6/2-NSE M17Z mice. Disease onset was scored as the first date when coarse coating or limb tremors were detected. Mice were scored three times per week by two trained observers blinded to the genotype and age of the mice. Disease onset and mortality were significantly delayed in the R6/2-NSE M17Z mice by 7.3 days and 20.4 days, respectively, when compared to R6/2 littermates (Fig. 1f). The protection conferred by M17Z expression represents a 55% increase in disease duration and a 20% prolongation of life. In addition, to rule out a strain-related epigenetic effect mediating protection, we treated seven-week-old R6/2 mice with the caspase inhibitor zVAD-fmk by continuous intracerebroventricular infusion for four weeks. zVAD-fmk-treated mice performed better on RotaRod (Fig. 2a) and lived 25% longer (98.6 versus 79.0 days, $n = 5$/group, $P = 0.002$) (Fig. 2b) than control mice treated with zFA-fmk.

There is controversy about the role of NII in Huntington's disease[4,6,14]. There is a close temporal relationship between NII detection and disease onset[4,6]. The appearance of NII is significantly delayed in R6/2-NSE M17Z mice when compared to R6/2 littermates. Nine-week-old R6/2 mice showed abnormal motor symptoms and abundant NII, as determined by ubiquitin and amino-terminal huntingtin immunohistochemistry (Fig. 3a, c), whereas R6/2-NSE M17Z mice were asymptomatic at nine weeks, and none had NII (Fig. 3b, d). NII were detected in twelve-week-old symptomatic R6/2-NSE M17Z mice (Fig. 3f). These results were replicated using two separate N-terminal huntingtin antibodies. Reactive fibrillary astrogliosis has been described as a significant finding in the brains of human patients. Reactive astrogliosis was detected in the cortex and striatum of nine-week-old R6/2 mice, as graded by a blinded neuropathologist (J.P.V.). Slight reactive astrogliosis was detected in one out of four age-matched R6/2-NSE M17Z mice, and none was detected in the other three R6/2-NSE M17Z mice or in the wild-type or NSE M17Z mice ($n = 4$ per genotype) (Fig. 3g, h).

There is an age-dependent decrease in neurotransmitter receptor binding and messenger RNA levels in R6/2 mice[5]. This decrease in adenosine A2a, dopamine D1 and dopamine D2 receptor binding and dopamine D2 receptor mRNA in R6/2 mice is significantly inhibited in R6/2-NSE M17Z mice (Fig. 4a). Functional deterioration in these mice correlated with the decrease in neurotransmitter density[5], so the improved functional status of the R6/2-NSE M17Z mice compared with the R6/2 mice is probably due in part to the delay in neurotransmitter-receptor loss. The densities of adenosine A2a, dopamine D1 and dopamine D2 receptors were not statistically significantly different between NSE M17Z and wild-type littermate mice.

Caspase-1 cleaves mutant and wild-type huntingtin *in vitro*[15]. To investigate the mechanism underlying the protection conferred by mutant caspase-1, we evaluated cleavage of endogenous huntingtin using a well characterized carboxy-terminal huntingtin antibody[16]. Compared to wild-type and NSE-M17Z mice, nine-week-old R6/2 mice show differential processing of huntingtin, with a prominent cleavage product revealed by western blotting. R6/2-NSE M17Z mice, on the other hand, do not show the cleavage band seen in R6/2 mice (Fig. 4b). Immunohistochemistry for endogenous huntingtin[17] showed diminished staining in the hippocampus, striatum, cortex and cerebellum of R6/2 mice as compared to wild-type and R6/2-NSE M17Z mice (Fig. 4c–k). The specific role of huntingtin cleavage fragments in Huntington's disease and in the formation of NII remains controversial. However, as cleavage of

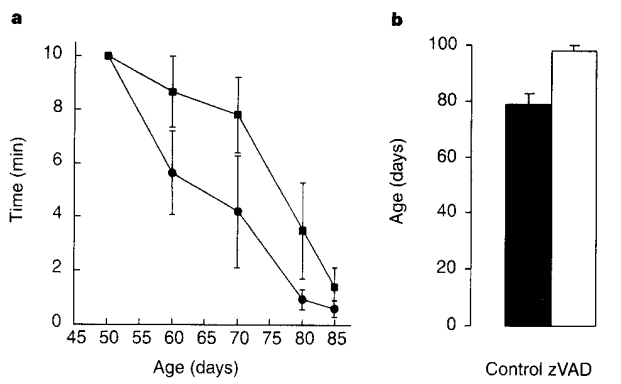


Figure 2 zVAD-fmk delays progression and mortality in R6/2 mice. **a**, Control zFA-fmk (circles) and zVAD-fmk (squares, treated R6/2 mice were tested on the RotaRod (15 r.p.m.), beginning the day before the placement of osmotic pumps for intracerebroventricular drug administration. **b**, Intracerebroventricular administration of zVAD-fmk delays mortality in P6 2 mice ($n = 5$ per group, $P < 0.0002$).

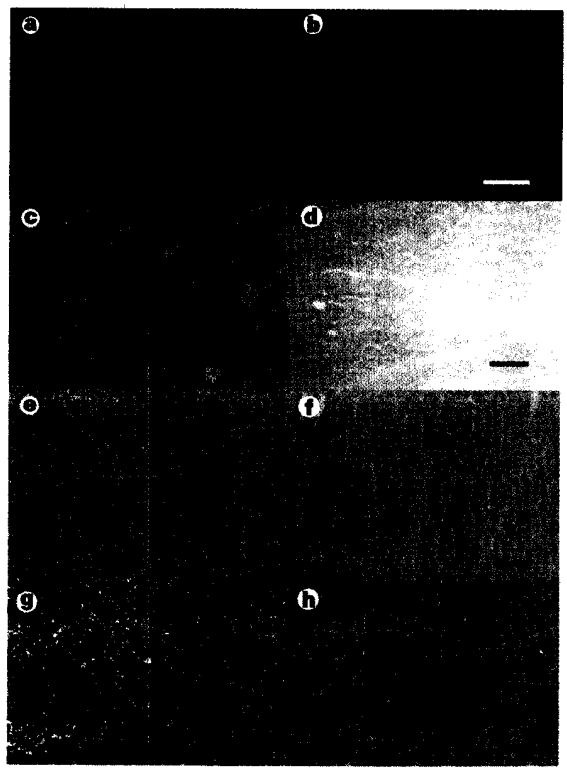


Figure 3 NII and astrogliosis are inhibited in R6/2-NSE M17Z mice. **a**, **b**, Fluorescent immunohistochemistry demonstrating ubiquitin-positive inclusions in the CA1 region of hippocampus in 9-week-old R6/2 mice (**a**), but not in R6/2-NSE M17Z mice (**b**). Scale bar, 50 μm. **c**, **d**, Peroxidase immunohistochemistry with EM48, an antibody directed against the N-terminal region of huntingtin, demonstrates NII in the striatum of 9-week-old R6/2 mice (**c**) but not of R6/2-NSE M17Z mice (**d**). Scale bar, 40 μm. **e**, **f**, At 12 weeks of age, ubiquitin-positive NII are present in the striatum of both R6/2 (**e**) and R6/2-NSE M17Z (**f**) mice, although the inclusions in the R6/2-NSE M17Z mice are smaller. Scale bar, 40 μm. **g**, **h**, Glial fibrillary acidic protein (GFAP) immunohistochemistry (brown peroxidase product with blue haematoxylin counterstain) in the hippocampal dentate region of 9-week-old R6/2 mice (**g**), and R6/2-NSE M17Z mice (**h**). Scale bar, 40 μm.

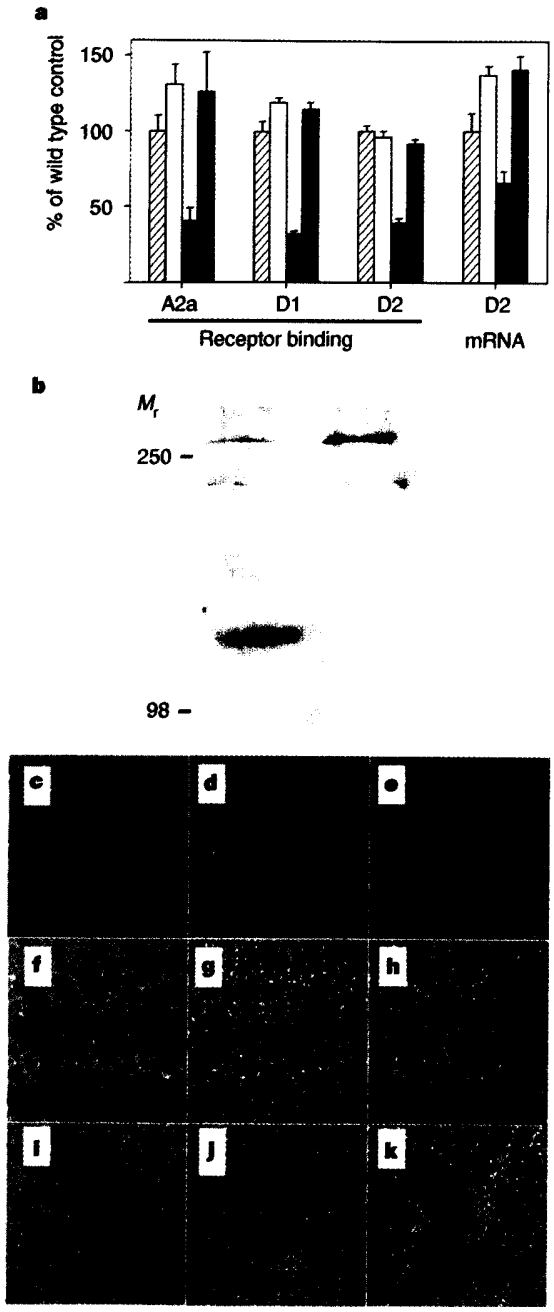


Figure 4 NSE M17Z inhibits neurotransmitter-receptor loss and cleavage of endogenous huntingtin in R6/2 mice. **a**, R6/2 mice have specific decreases in neurotransmitter-receptor binding preceded by decreases in corresponding mRNA species[5]. At nine weeks of age, R6/2 mice (black bars) had significantly less receptor binding than wild-type (hatched bars), NSE M17Z (white bars) or R6/2 NSE M17Z (shaded bars) mice. In addition, R6/2 mice had significantly less dopamine-D2-receptor mRNA than other groups of mice (analysis of variance, $P < 0.05$ for all assays). Baseline differences between wild-type and NSE-M17Z receptor levels were not statistically significant. **b**, Western-blot analysis using an antibody against amino acids 1,981-2,580 of human huntingtin[16] shows differential processing of endogenous huntingtin in R6/2 (left lane) and R6/2-NSE M17Z (right lane) mice. Relative molecular mass markers are shown on the left (in thousands). **c**-**k**, Peroxidase immunohistochemistry using the same anti-huntingtin antibody[17] in the Purkinje-cell layer of the cerebellum (**c**, **d**, **e**), frontal cortex (**f**, **g**, **h**) and striatum (**i**, **j**, **k**) in wild-type (**c**, **f**, **i**), R6/2 (**d**, **g**, **j**) and R6/2-NSE M17Z (**e**, **h**, **k**) mice. R6/2 mice consistently demonstrate reduced immunoreactivity for endogenous huntingtin, as compared to wild-type and R6/2-NSE M17Z mice.

wild-type and mutant huntingtin *in vitro* by caspase-1 has been demonstrated, the above evidence implicates caspase-1 in the generation of wild-type and mutant huntingtin fragments *in vivo*[15]. Apoptotic features have been described in striatal cells transfected with wild-type full-length *huntingtin*[18].

We demonstrate that motor weakness, NII formation, neurotransmitter receptor alteration and, most important, symptomatic onset and mortality in R6/2 mice is delayed by expression of a dominant-negative caspase-1 mutant. In addition, we have delayed mortality of R6/2 mice by chronic intracerebroventricular administration of a caspase inhibitor. We propose that caspases inhibitable by mutant caspase-1 are important in the Huntington's disease-like phenotype of the R6/2 transgenic mouse. Elevation of mature IL-1β levels in symptomatic R6/2 mice, which was inhibited in R6/2-NSE M17Z mice, indicates that caspase-1 may be critical for the symptomatic disease progression of R6/2 mice. In addition, detection of increased mature IL-1β in the brains of Huntington's disease patients adds significance to these findings. Reductions in specific neuronal populations have been identified in R6/2 mice of more than 12 weeks old (S. Davies, personal communication). However, neuronal dysfunction appears to be the dominant factor mediating the appearance of symptoms and death in the R6/2 mouse[3,5]; lack of significant cell loss is probably secondary to rapid disease progression, which does not allow significant cell death to occur[3]. Evidence for apoptosis has been seen in Huntington's disease patients and *in vitro* using transfection with mutant *huntingtin*[14,19,20]. In addition, a transgenic mouse expressing full-length huntingtin shows significant apoptotic neurodegeneration and behavioural characteristics of Huntington's disease[21]. As the expression of this dominant-negative caspase-1 mutant delays neuronal dysfunction as well as death, our data implicate caspase-1-mediated pathways in the symptomatic progression of R6/2 mice. Although R6/2 mice have diabetes[22], which probably affects body weight, the presence of NII and alterations in neurotransmitter receptors are unlikely to be related to diabetic effects.

In acute cellular injury, such as ischaemia, caspases are activated sufficiently to mediate cell death[8,11,23]. In a chronic neurodegenerative disease, certain caspases may be activated at a sub-lethal threshold, insufficient to cause cell death but enough to cause cellular abnormalities, manifested in R6/2 mice as neuronal dysfunction. These results indicate a novel role for caspase-1 not only in cell death, but also in mediating cellular dysfunction leading to symptomatic progression and death. Caspase-1 and caspase-3 (but not caspase-7 or caspase-8) cleave huntingtin, and caspase-1 can activate caspase-3 *in vitro*[15,24,25]. Given that endogenous murine huntingtin is cleaved in R6/2 symptomatic mice, one possible mechanism is that the mutant exon 1 of *huntingtin* initiates a toxic state within susceptible neuronal populations, leading to caspase-1 activation and cleavage of certain proteins, including huntingtin. Caspase-1 could also activate caspase-3, mediating further cleavage of endogenous huntingtin and increasing the concentration of small huntingtin fragments, accelerating the formation of NII.

This study provides *in vivo* functional mechanistic evidence of caspase-1 activation mediated by exon 1 of mutant *huntingtin*. Caspase-1 mediates pro-IL-1β processing, generating secreted mature IL-1β (ref. 26). Endogenously produced mature IL-1β is involved in neuronal cell death[27,28], and reactive astrogliosis, which occurs as a response to cellular injury, is stimulated by IL-1β[29]. The precise relationship of IL-1β and astrogliosis to the progression of Huntington's disease is still unclear. Caspase-1-mediated pathways appear to be shared in a variety of acute and chronic neurological disorders (ischaemia, ALS, Huntington's disease and Parkinson's disease) as a common mechanism mediating cell dysfunction and cell death[8,12,23,30]. Our findings show that caspase-1 plays an important and specific role in the early stages of Huntington's disease, as demonstrated by the inhibition of both NII formation and the specific neuroreceptor abnormalities found in the disease. Caspase-1

inhibition delays onset and prolongs survival in a transgenic mouse model of Huntington's disease, and is potentially applicable to the human disease. □

Methods

Animals. Four male NSE M17 mice were crossed with eight wild-type female recipients of transplanted ovaries from R6/2 mice (Jackson Laboratories). Polymerase chain reaction was used for genotyping[3,8]. We used complete consecutive litters up to a certain birth date for symptomatic studies. Litters generated thereafter were used for the remaining studies.

Mature IL-1β determination. Mature IL-1β quantification was done as previously described using an ELISA kit (Genzyme)[23].

Intracerebroventricular implantation of osmotic pumps. Spontaneously breathing seven-week-old R6/2 mice were anaesthetized, and a 2-cm sagittal incision was made over the skull. A small opening was made on the cranium 1 mm right lateral to the bregma. A microcannula was inserted to a depth of 3 mm, secured with a dental acrylic (Duralay, Bioanalytical Systems), and attached to an osmotic pump (Alzet). The pump was prefilled with 100 μg per 20 g body weight of either zVAD-fmk or zFA-fmk (Enzyme Systems). The pumps continuously deliver the drug for four weeks. The experimenter was blinded to the identity of the drug used in the pump until the death of all the mice.

***In situ* hybridization.** We constructed oligonucleotide probes targeted against a human-specific intron of the human Huntington's disease transgene sequence (sequence 5′-TCT GGG TTG CTG GGT CAC TCT GTC TCT GCG GAG CCG GGG G-3′) and against the dopamine-D2-receptor gene (sequence 5′-GGC AGG GTT GGC AAT GAT ACA CTC ATT CTG GTC TGT ATT-3′). Probes were 3′-end labelled with ^{35}S-dATP using an oligonucleotide-labelling kit (NEN Life Science Products). Parasagittal sections (12 μm) of frozen mouse brains were thaw-mounted onto poly-L-lysine-coated glass slides. Slides were fixed in 4% paraformaldehyde/0.1 M phosphate buffered-saline (PBS) for 10 min, washed in PBS for 3 × 5 min, acetylated with 0.25% acetic anhydride in 0.1 M triethanolamine, pH 8.0, for 10 min, washed in PBS for 5 min, and dehydrated in graded ethanol solutions. Slides were incubated overnight at 37 °C with 80 μl of hybridization buffer (50% formamide, 0.3 M NaCl, 10 mM Tris, 1 mM EDTA, 10% dextran sulphate, 1× Denhart's solution) containing radioactively labelled probe (30,000 c.p.m. per μl). After hybridization, slides were washed in a series of sodium citrate–sodium chloride washes, rinsed with 70% ethanol and air-dried. The slides were apposed to β-max film (Amersham) and exposed for 2 weeks before the film was developed. Film densities were analysed using a computer-based image-analysis system (M1, Imaging Research).

Neuronal intranuclear inclusion and neurotransmitter receptor analysis. Receptor binding was done in parallel on fresh frozen brain tissue from wild-type, NSE M17Z, R6/2 and R6/2-NSE M17Z mice ($n = 4$ animals per group) as described[5]. Immunohistochemistry was performed on 12-μm brain sections using antibodies against ubiquitin (Dako), glial fibrillary acidic protein or huntingtin[16] as described[17]. Western blotting was done according to standard techniques using an anti-huntingtin antibody (HF-1; courtesy of M. MacDonald).

Received 22 February; accepted 14 April 1999.

1. Harper, P. S. *Huntington's Disease* (Saunders, London, 1991).
2. Huntington's Disease Collaborative Research Group. A novel gene containing a trinucleotide repeat that is unstable on Huntington's disease chromosomes. *Cell* **72,** 971–983 (1993).
3. Mangiarini, L. *et al.* Exon 1 of the HD gene with an expanded CAG repeat is sufficient to cause a progressive neurological phenotype in transgenic mice. *Cell* **87,** 493–506 (1996).
4. Davies, S. W. *et al.* Formation of neuronal intranuclear inclusions underlies the neurological dysfunction in mice transgenic for the HD mutation. *Cell* **90,** 537–548 (1997).
5. Cha, J. H. *et al.* Altered brain neurotransmitter receptors in transgenic mice expressing a portion of an abnormal human huntington disease gene. *Proc. Natl Acad. Sci. USA* **95,** 6480–6485 (1998).
6. DiFiglia, M. *et al.* Aggregation of huntingtin in neuronal intranuclear inclusions and dystrophic neurites in brain. *Science* **277,** 1990–1993 (1997).
7. Alnemri, E. S. *et al.* Human ICE/CED-3 protease nomenclature. *Cell* **87,** 171 (1996).
8. Friedlander, R. M. *et al.* Expression of a dominant negative mutant of interleukin-1 beta converting enzyme in transgenic mice prevents neuronal cell death induced by trophic factor withdrawal and ischemic brain injury. *J. Exp. Med.* **185,** 933–940 (1997).
9. Forss-Petter, S. *et al.* Transgenic mice expressing beta-galactosidase in mature neurons under neuron-specific enolase promoter control. *Neuron* **5,** 187–197 (1996).
10. Burne, J. F., Staple, J. K. & Raff, M. C. Glial cells are increased proportionally in transgenic optic nerves with increased numbers of axons. *J. Neurosc.* **16,** 2064–2073 (1996).
11. Hara, H. *et al.* Attenuation of transient focal cerebral ischemic injury in transgenic mice expressing a mutant ICE inhibitory protein. *J. Cereb. Blood Flow Metab.* **17,** 370–375 (1997).
12. Friedlander, R. M., Brown, R. H., Gagliardini, V., Wang, J. & Yuan, J. Inhibition of ICE slows ALS in mice. *Nature* **388,** 31 (1997).
13. Li, P. *et al.* Mice deficient in IL-1 beta-converting enzyme are defective in production of mature IL-1 beta and resistant to endotoxic shock. *Cell* **80,** 401–411 (1995).
14. Saudou, F., Finkbeiner, S., Devys, D. & Greenberg, M. E. Huntingtin acts in the nucleus to induce apoptosis but death does not correlate with the formation of intranuclear inclusions. *Cell* **95,** 55–66 (1998).
15. Wellington, C. L. *et al.* Caspase cleavage of gene products associated with triplet expansion disorders generates truncated fragments containing the polyglutamine tract. *J. Biol. Chem.* **273,** 9158–9167 (1998).
16. Persichetti, F. *et al.* Differential expression of normal and mutant Huntington's disease gene alleles. *Neurobiol. Dis.* **3,** 183–190 (1996).
17. Kosinski, C. M. *et al.* Huntingtin immunoreactivity in the rat neostriatum: differential accumulation in the projection and interneurons. *Exp. Neurol.* **144,** 239–247 (1997).
18. Kim, M. *et al.* Mutant huntingtin expression in clonal striatal cells: dissociation of inclusion formation and neuronal survival by caspase inhibition. *J. Neurosci.* **19,** 964–973 (1999).
19. Portera-Cailliau, C., Hedreen, J. C., Price, D. L. & Koliatsos, V. E. Evidence for apoptotic cell death in Huntington disease and excitotoxic animal models. *J. Neurosci.* **15,** 3775–3787 (1995).
20. Lunkes, A. & Mandel, J. L. A cellular model that recapitulates major pathogenic steps of Huntington's disease. *Hum. Mol. Genet.* **7,** 1355–1361 (1998).
21. Reddy, P. H. *et al.* Behavioural abnormalities and selective neuronal loss in HD transgenic mice expressing mutated full-length HD cDNA. *Nature Genet.* **20,** 198–202 (1998).
22. Hurlbert, M. S. *et al.* Mice transgenic for an expanded CAG repeat in Huntington's disease gene develop diabetes. *Diabetes* **8,** 649–651 (1999).
23. Hara, H. *et al.* Inhibition of interleukin 1beta converting enzyme family proteases reduces ischemic and excitotoxic neuronal damage. *Proc. Natl Acad. Sci. USA* **94,** 2007–2012 (1997).
24. Goldberg, Y. P. *et al.* Cleavage of huntingtin by apopain, a proapoptotic cysteine protease, is modulated by the polyglutamine tract. *Nature Genet.* **13,** 442–449 (1996).
25. Tewari, M. *et al.* Yama/CPP32 beta, a mammalian homolog of CED-3, is a CrmA-inhibitable protease that cleaves the death substrate poly(ADP-ribose) polymerase. *Cell* **81,** 801–809 (1995).
26. Thornberry, N. A. *et al.* A novel heterodimeric cysteine protease is required for interleukin-1 beta processing in monocytes. *Nature* **356,** 768–774 (1992).
27. Troy, C. M., Stefanis, L., Prochiantz, A., Greene, L. A. & Shelanski, M. L. The contrasting roles of ICE family proteases and interleukin-1beta in apoptosis induced by trophic factor withdrawal and by copper/zinc superoxide dismutase down-regulation. *Proc. Natl Acad. Sci. USA* **93,** 5635–5640 (1996).
28. Friedlander, R. M., Gagliardini, V., Rotello, R. J. & Yuan, J. Functional role of interleukin 1 beta (IL-1 beta) in IL-1 beta-converting enzyme-mediated apoptosis. *J. Exp. Med.* **184,** 717–724 (1996).
29. Lee, S. C., Dickson, D. W. & Brosnan, C. F. Interleukin-1, nitric oxide and reactive astrocytes. *Brain Behav. Immun.* **9,** 345–354 (1995).
30. Klivenyi, P., Andreassen, O., Friedlander, R. M. & Beal, M. F. Transgenic mice expressing a dominant negative mutant interleukin-1b converting enzyme shows resistance to MPTP neurotoxicity. *NeuroReport* **10,** 635–638 (1999).

Acknowledgements. We thank E. Signer for advice and support; C. Swap, A. Dunah and W. Hobbs for expert technical assistance; M. MacDonald for providing Huntingtin antibodies; and E. Balodimas for editorial assistance. This work was supported by a grant from the Hereditary Disease Foundation (to R.M.F. and J.H.J.C.), the Huntington's Disease Society of America (to J.-H.J.C.), the Glendorn Foundation (to A.B.Y.) and by grants from the NIH (to J.-H.J.C., A.B.Y. and J.Y.). This paper is dedicated to J.B.P., who died during the review of this manuscript.

Correspondence and requests for materials should be addressed to R.M.F. (e-mail: rfriedlander@rics.bwh.harvard.edu).

In vivo cell sorting in complementary segmental domains mediated by Eph receptors and ephrins

Qiling Xu, Georg Mellitzer, Vicky Robinson & David G. Wilkinson

Division of Developmental Neurobiology, National Institute for Medical Research, The Ridgeway, Mill Hill, London NW7 1AA, UK

The restriction of intermingling between specific cell populations is crucial for the maintenance of organized patterns during development. A striking example is the restriction of cell mixing between segments in the insect epidermis[1] and the vertebrate hindbrain[2] that may enable each segment to maintain a distinct identity. In the hindbrain, this is a result of different adhesive properties of odd- and even-numbered segments (rhombomeres)[3,4], but an adhesion molecule with alternating segmental expression has not been found. However, blocking experiments suggest that Eph-receptor tyrosine kinases may be required for the segmental restriction of cells[5]. Eph receptors and their membrane-bound ligands, ephrins, are expressed in complementary rhombomeres[6] and, by analogy with their roles in axon pathfinding[7,8], could mediate cell repulsion at boundaries. Remarkably, transmembrane ephrins can themselves transduce signals[9,10], raising the possibility that bi-directional signalling occurs between adjacent ephrin- and Eph-receptor-expressing